

## Asymmetric Activated Carbon-Manganese Dioxide Capacitors in Mild Aqueous Electrolytes Containing Alkaline-Earth Cations

Chengjun Xu, Hongda Du, Baohua Li, Feiyu Kang and Yuqun Zeng

*J. Electrochem. Soc.* 2009, Volume 156, Issue 6, Pages A435-A441.  
doi: 10.1149/1.3106112

---

**Email alerting  
service**

Receive free email alerts when new articles cite this article - sign up in the box at the top right corner of the article or [click here](#)

---

---

To subscribe to *Journal of The Electrochemical Society* go to:  
<http://jes.ecsdl.org/subscriptions>

---

© 2009 ECS - The Electrochemical Society



## Asymmetric Activated Carbon-Manganese Dioxide Capacitors in Mild Aqueous Electrolytes Containing Alkaline-Earth Cations

Chengjun Xu,<sup>a,b</sup> Hongda Du,<sup>a</sup> Baohua Li,<sup>a</sup> Feiyu Kang,<sup>b,z</sup> and Yuqun Zeng<sup>c</sup>

<sup>a</sup>Advanced Materials Institute, Graduate School at Shenzhen, Tsinghua University, Shenzhen City, Guangdong Province 518055, China

<sup>b</sup>Laboratory of Advanced Materials, Department of Materials Science and Engineering, Tsinghua University, Beijing 100084, China

<sup>c</sup>Amperex Technology Limited, Dongguan City, Guangdong Province 523080, China

Manganese dioxide exhibits the ideal capacitive behavior in aqueous electrolytes containing alkaline-earth cations ( $\text{Mg}^{2+}$ ,  $\text{Ca}^{2+}$ , or  $\text{Ba}^{2+}$ ). A specific capacitance value as high as  $325 \text{ F g}^{-1}$  was obtained in  $0.1 \text{ mol L}^{-1} \text{ Mg}(\text{NO}_3)_2$  electrolyte at  $2 \text{ mV s}^{-1}$ . The ideal capacitive behavior, high specific capacitance, good coulombic efficiency, and rate ability of manganese dioxides in aqueous electrolytes containing bivalent cations ( $\text{Mg}^{2+}$ ,  $\text{Ca}^{2+}$ , or  $\text{Ba}^{2+}$ ) indicate that these alkaline-earth cations might be good alternatives for the state-of-the-art univalent alkaline cations. Moreover, activated carbon/ $\text{MnO}_2$  asymmetric capacitors with  $2 \text{ V}$  operating voltage were built up based on the aqueous electrolytes containing these alkaline-earth cations. The energy density of the AC/ $\text{MnO}_2$  asymmetric capacitor with  $\text{Ca}^{2+}$  cation at a current density of  $0.3 \text{ A g}^{-1}$  was found to be  $21 \text{ Wh Kg}^{-1}$ . © 2009 The Electrochemical Society. [DOI: 10.1149/1.3106112] All rights reserved.

Manuscript submitted December 22, 2008; revised manuscript received February 16, 2009. Published April 7, 2009.

The electrochemical capacitor (supercapacitor) is an attractive device to be used solely or auxiliary as the power supply for electric vehicles or electronic products. Due to the fast pace of expansion of human activity, the need for supercapacitors with high energy and power densities as well as low cost and environmental friendliness is obvious and urgent. Because it does not need specific manufacturing conditions, the solvent (water) is low cost and totally nontoxic, and the aqueous electrolytes possess relatively high conductivity, aqueous-based activated carbon (AC) symmetric supercapacitors are promising low cost devices for providing high power densities.<sup>1</sup> However, the energy density of such a device is relatively low due to the limited cell voltage. The energy density ( $E$ ) of a supercapacitor is proportional to the capacitance ( $C$ ) and the voltage ( $V$ ) as follows

$$E = CV^2/2 \quad [1]$$

Due to the limitation of the water decomposition, the aqueous-based carbon symmetric supercapacitor only works in a maximum window of  $1 \text{ V}$ . According to Eq. 1, the relatively low energy density precludes its use in the industrial scale.<sup>1</sup>

An efficient way to improve the cell voltage in terms of the energy density is to use organic electrolytes with a wider electrochemical stability window than water.<sup>1</sup> Organic electrolytes including the combination of a solvent with different salts could enable the maximum cell voltage to reach more than  $3 \text{ V}$ , a value three times than the maximum cell voltage of aqueous-based supercapacitors.<sup>1-3</sup> However, such improvements inevitably sacrifice the capacitance and equivalent series resistance, which precludes it from easily reaching-high power density.<sup>1,4,5</sup> The organic electrolytes also suffer from highly toxic, flammable, or safety hazards. In addition, due to a water-free fabrication environment and the high prices of the solvents and salts, the manufacturing costs are also high for such devices.<sup>1</sup> Therefore, it is clear that the aqueous-based supercapacitors would be more attractive from cost, safety, and environmentally friendly points of view, but it is necessary to improve the energy density dramatically. Based on Eq. 1, there are two obvious methods to improve the energy density as well as the power density by using large capacitance electrode materials and increasing cell voltage. The low voltage could be partially compensated by the use of the pseudo-capacitive materials with a high capacitance, such as  $\text{RuO}_2$ .<sup>6,7</sup> The so-called pseudo-capacitive properties of a material were characterized with the rectangular cyclic voltammograms and

the linear variation of the potential on the time at a constant current charge or discharge, where the mechanism for energy storage is based on the faradaic reactions between the electrode and the electrolyte instead of the electrochemical double-layer mechanism.<sup>1</sup> During the last few years, various metal oxides have been proposed for pseudo-capacitance purpose. Among them,  $\text{RuO}_2$  presents the best performance ( $860 \text{ F g}^{-1}$ ) in  $\text{H}_2\text{SO}_4$  electrolyte.<sup>6,7</sup> However, ruthenium is a noble metal, which limits its use on a large scale.

Another strategy is to increase the cell voltage to more than  $1 \text{ V}$  by a smart asymmetric configuration. The so-called asymmetric or hybrid configurations combining two kinds of electrode materials in the same cell utilize the different potential windows of the different electrode materials in the same electrolyte to obtain a high cell voltage. For the asymmetric or hybrid AC/metal oxide electrochemical supercapacitors, one electrode stores charge through a reversible, nonfaradaic reaction of ion adsorption/desorption on the surface of an active carbon, and the other electrode utilizes a reversible redox faradaic reaction in a transition metal oxide or a lithium-ion intercalated compound. AC/ $\text{Ni}(\text{OH})_2$  and AC/ $\text{LiMn}_2\text{O}_4$  aqueous cells are two typical representatives,<sup>8-11</sup> in which not only a much higher voltage (more than  $1.5 \text{ V}$ ) could be achieved but also a higher capacitance material was introduced to replace one AC electrode. Due to the remarkable performance, more attention has been paid to these AC/metal oxide aqueous supercapacitors. Recently, AC/manganese dioxide ( $\text{MnO}_2$ ) capacitors using aqueous electrolytes containing alkaline cations have become another hot spot in this area due to the high operating voltage (more than  $2 \text{ V}$ ) and nontoxicity and low cost of manganese dioxides as well as the safety and non-erosion of the mild electrolytes.<sup>12-15</sup>

Manganese dioxides are promising electrode materials exhibiting ideal capacitive behavior in aqueous mild electrolytes containing alkaline cations ( $\text{Li}^+$ ,  $\text{Na}^+$ , or  $\text{K}^+$ ) with a potential width ranging from  $0.9$  to  $1.2 \text{ V}$ .<sup>12-15</sup> The charge storage mechanism of manganese dioxides is based on the double injection and ejection of cations and electrons, in which the cations ( $\text{Li}^+$ ,  $\text{Na}^+$ , or  $\text{K}^+$ ) intercalate into  $\text{MnO}_2$  lattice and correspondingly  $\text{Mn}(\text{IV})$  becomes  $\text{Mn}(\text{III})$  to balance the charge.<sup>16-22</sup> One univalent alkaline cation inserted into  $\text{MnO}_2$  and one electron are stored. More recently, the polyvalent cations intercalation process of  $\text{MnO}_2$  has been investigated in our lab.<sup>22</sup> Our previous work<sup>22</sup> indicated that  $\text{MnO}_2$  showed ideal capacitive behavior in the aqueous solution containing bivalent cations ( $\text{Ca}^{2+}$ ), and the specific capacitance has been improved dramatically only through the use of polyvalent cations ( $\text{Ca}^{2+}$ ) in place of traditional univalent cations ( $\text{Na}^+$ ). From the fundamental point of view, the polyvalent cations are advantageous because each polyvalent

<sup>z</sup> E-mail: fykang@tsinghua.edu.cn

**Table I. Ionic radii, ionic conductivity, and standard redox potential of alkaline and alkaline-earth cations.<sup>23</sup>**

		Li <sup>+</sup>	Na <sup>+</sup>	K <sup>+</sup>	Mg <sup>2+</sup>	Ca <sup>2+</sup>	Ba <sup>2+</sup>
Size (Å)	In crystals	0.69	1.02	1.38	0.66	0.99	1.34
	In aqueous solution	6	4	3	8	5	6
Standard redox potential (V)		-3.05	-2.71	-2.93	-2.38	-2.84	-2.92

cation intercalated into a host compound results in a concurrent charge transfer of two or even three electrons to the host material. Other alkaline earth cations (Mg<sup>2+</sup> and Ba<sup>2+</sup>) possess a similar electron structure and close ion size as well as a close standard redox potential with alkaline cations (Li<sup>+</sup> and K<sup>+</sup>),<sup>23</sup> as shown in Table I, which is widely used in the aqueous electrolytes for MnO<sub>2</sub> supercapacitors. Therefore, Mg<sup>2+</sup> and Ba<sup>2+</sup> ions may be the other good guest polyvalent cations for MnO<sub>2</sub> supercapacitors just like Ca<sup>2+</sup> ion. Thus, this work first aims to address the ideal capacitive behavior of MnO<sub>2</sub> in the aqueous systems containing alkaline earth cations (Mg<sup>2+</sup>, Ca<sup>2+</sup>, and Ba<sup>2+</sup>). The ideal capacitive behavior, high specific capacitance, high reversibility, and good rate ability indicate that alkaline-earth cations (Mg<sup>2+</sup>, Ca<sup>2+</sup>, and Ba<sup>2+</sup>) are promising alternatives for the traditional alkaline cations.

Second, MnO<sub>2</sub> only shows the ideal capacitive behavior in aqueous electrolytes within a potential window of 0.9 V.<sup>12-15</sup> Unfortunately, this potential window is relatively smaller than organic-based capacitors, and consequently MnO<sub>2</sub>-based capacitors deliver limited power or energy densities. The best way to overcome this drawback is to utilize the asymmetric assemblies, in which MnO<sub>2</sub> and AC are used as positive and negative electrodes in the presence of aqueous electrolytes containing alkaline-earth cations (Mg<sup>2+</sup>, Ca<sup>2+</sup>, or Ba<sup>2+</sup>). This configuration also enables the operating voltage of the asymmetric supercapacitors in mild electrolytes containing alkaline-earth cations to reach 2 V. In addition, combined with the improved specific capacitance of the positive electrode due to the usage of alkaline-earth cations, good performance of these asymmetric devices was reported in this work.

Last, the size of the cation, the size of the hydrated cation, the mobility of the cation, and the adsorption-desorption rate may have a direct impact on the pseudo-capacitive behaviors of manganese dioxide as well as the double-layer capacitive behavior of negative AC. Therefore, the role of cation species on the electrochemical properties of positive manganese dioxide and negative AC as well as the performance of the asymmetric AC/MnO<sub>2</sub> cells is pursued in this work.

### Experimental

**Preparation of positive MnO<sub>2</sub> electrode.**— A MnO<sub>2</sub> sample was prepared by a self-reacting microemulsion. A surfactant of 13.32 g of sodium bis(2-ethylhexyl) sulfosuccinate (AOT) was added in 300 mL iso-octane and stirred well to get an AOT/iso-octane solution. Then, 32.4 mL of 0.1 mol L<sup>-1</sup> (M) KMnO<sub>4</sub> aqueous solution was added and this solution was dispersed by ultrasound for 30 min to prepare a dark brown precipitate. The product was separated, washed copiously several times with distilled water and ethanol, and dried at 80°C for 12 h. Our previous works<sup>24,25</sup> indicated that the as-prepared MnO<sub>2</sub> sample possesses a spherical morphology with an individual particle size of around 4 nm. N<sub>2</sub> adsorption and desorption measurement indicated that the S<sub>BET</sub> value of the as-prepared sample is 145 m<sup>2</sup> g<sup>-1</sup>. A commercial AC was used as the negative electrode material.

**Single electrode measurements.**— Electrodes were prepared by mixing 70 wt % of MnO<sub>2</sub> powder as active material with 20 wt % acetylene black and 10 wt % polytetrafluoroethylene (PTFE). MnO<sub>2</sub> powder (70 mg) and acetylene black (20 mg) were first mixed and dispersed in ethanol by ultrasound for 30 min. Then, the ink was dried at 80°C for 4 h to get a dark mixed powder, and 10 mg of PTFE was added to get a paste. Then, the paste was dried at 80°C,

and a little 1-methy-2-pyrrolidinone (NMP) was added to get a syrup. The syrup was cold rolled into thick films, and pieces of film 5 mg in weight and 1 cm<sup>2</sup> in size were then hot-pressed at 80°C under 100 MPa on a titanium plate. The preparation process of the negative AC electrode was similar to the process of MnO<sub>2</sub> electrode, except that the weight ratio of AC power to acetylene black to binder was 8:1:1. Electrochemical tests were performed with an Im6e (Zahner) electrochemical station. A piece of platinum gauze and a saturated calomel electrode (SCE) were assembled as the counter and reference electrode, respectively. A luggin capillary facing the working electrode at a distance of 2 mm was used to minimize errors due to internal resistance (iR) drop in the electrolyte. Impedance measurements of MnO<sub>2</sub> electrodes were conducted at 0.4 V vs SCE by sweeping frequencies from 30 mHz to 50 KHz. The measured impedance data were analyzed using Zview software. In addition, the specific capacitance of acetylene black in all electrolytes was found to be negligible (less than 10 F g<sup>-1</sup>).

**Asymmetric capacitor.**— The capacitor test used the coin-cell assembly consisting of MnO<sub>2</sub> positive and AC negative electrodes. The MnO<sub>2</sub>/AC weight ratios were calculated by considering specific voltammetric charge and the appropriate potential window of positive and negative electrodes in different electrolytes. A glass paper was used as the separator. The titanium foil (50 μm in thickness) was used as the current collector. All the electrolytes were bubbled by N<sub>2</sub> gas for 30 min to eliminate oxygen before assembly.<sup>15</sup>

The real power density,  $P_{\text{real}}$ , and the real energy,  $E_{\text{real}}$ , were determined from the constant-current charge/discharge cycles as follows

$$P_{\text{real}} = \Delta EI/m \text{ (W/Kg)} \quad [2]$$

where  $\Delta E = (E_{\text{max}} - E_{\text{min}})/2$  with  $E_{\text{max}}$  the potential at the end of charge and  $E_{\text{min}}$  at the end of discharge,  $I$  is the applied current (A), and  $m$  is the total weight of positive and negative active material in the electrode (kg)

$$E_{\text{real}} = P_{\text{real}}t \text{ (Wh/kg)} \quad [3]$$

where  $t$  is the discharge time (h). Finally, the coulombic efficiency is given by the discharge time/charge time ratio.<sup>15</sup>

### Results and Discussion

**Electrochemical properties of positive MnO<sub>2</sub> electrode.**— Cyclic voltammetric tests of MnO<sub>2</sub> electrode were measured in 0.1 mol L<sup>-1</sup> Ca(NO<sub>3</sub>)<sub>2</sub> (pH 6.0) at 2 mV s<sup>-1</sup> with a wide potential range to investigate the reversibility of MnO<sub>2</sub> electrode by controlling the upper and lower potential limits. Figure 1 shows the cyclic voltammograms (CVs) at different potential ranges. It can be seen from curve 1 in Fig. 1 that for a potential more negative than about 0.1 V, the irreversible faradaic processes are observed and might correspond to the reduction of surface manganese dioxide. When the potential is more positive than 1.0 V, at ~1.05 V, an anodic wave is detected. In addition, the onset of the water oxidation is also observed at potentials more positive than ~1.3 V. As the potential is controlled from 0.10 to 1.00 V vs SCE, the shape of the CV is a nearly rectangular mirror image characteristic of the capacitive behavior, as shown in curve 2. The maximum and minimum values of polarization potential of MnO<sub>2</sub> electrode are controlled by the surface reactions Mn(IV) to Mn(II) and Mn(IV) to Mn(VII), respectively, which are irreversible because of the solubility of both Mn(II)

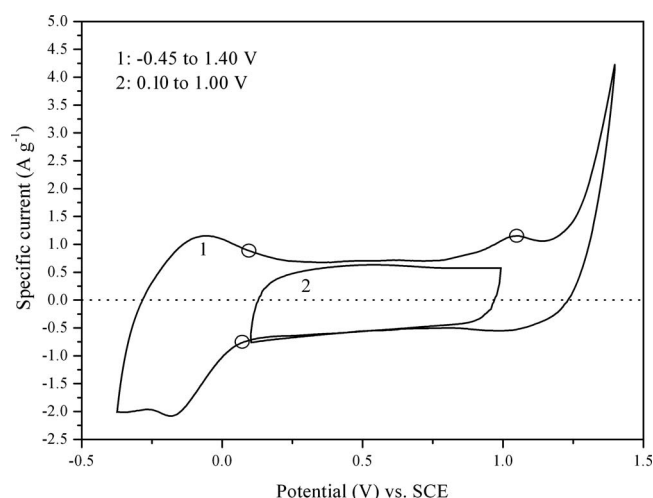


**Figure 1.** CVs of MnO<sub>2</sub> electrode in 0.1 mol L<sup>-1</sup> Ca(NO<sub>3</sub>)<sub>2</sub> at different potential ranges.

and Mn(IV) in water.<sup>13,25</sup> Therefore, the potential must be controlled in the region in which the reversible pseudo-capacitive behavior occurs.

Cyclic voltammetric tests have been performed on MnO<sub>2</sub> electrodes between 0.10 and 1.00 V vs SCE in 0.1 mol L<sup>-1</sup> (M) Mg(NO<sub>3</sub>)<sub>2</sub>, Ca(NO<sub>3</sub>)<sub>2</sub>, and Ba(NO<sub>3</sub>)<sub>2</sub> electrolytes (pH 6.0). Figure 2 shows the CVs at a sweep rate of 10 mV s<sup>-1</sup>. These profiles are relatively rectangular in shape, which indicates the ideal capacitive behavior. The specific capacitance (SC) of active material can be estimated using half the integrated area of the CV curve to obtain the charge (*Q*) and subsequently dividing the charge by the mass of the active material (*m*) and the width of the potential window ( $\Delta V$ )

$$SC = Q/\Delta Vm \quad [4]$$

The SC values in 0.1 M Mg(NO<sub>3</sub>)<sub>2</sub>, Ca(NO<sub>3</sub>)<sub>2</sub>, and Ba(NO<sub>3</sub>)<sub>2</sub> electrolytes at a low sweep rate of 2 mV s<sup>-1</sup> are 325, 314, and 281 F g<sup>-1</sup>, respectively. These values were much higher than 194 F g<sup>-1</sup> in 0.2 M NaNO<sub>3</sub> electrolyte (pH 6.0).<sup>22</sup> It is shown that the capacitance of MnO<sub>2</sub> has been improved dramatically only through replacing the traditional univalent cation by the bivalent alkaline-earth cations. This improvement method is the most efficient, low cost, and convenient way.

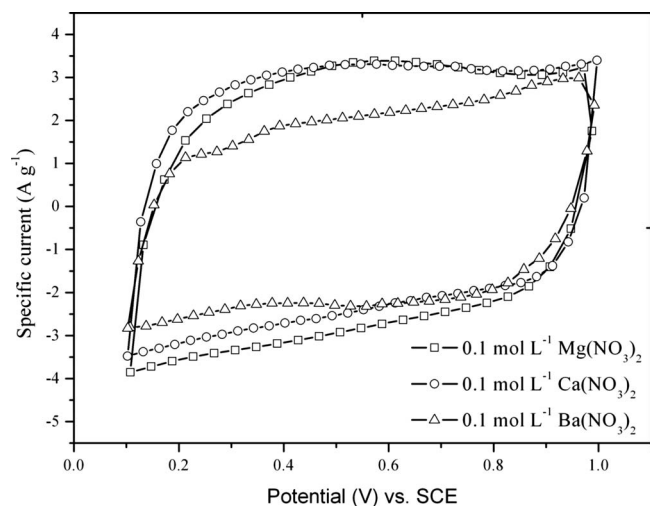


**Figure 2.** CVs of MnO<sub>2</sub> electrodes in 0.1 mol L<sup>-1</sup> Mg(NO<sub>3</sub>)<sub>2</sub>, Ca(NO<sub>3</sub>)<sub>2</sub>, and Ba(NO<sub>3</sub>)<sub>2</sub> electrolytes at 10 mV s<sup>-1</sup>.

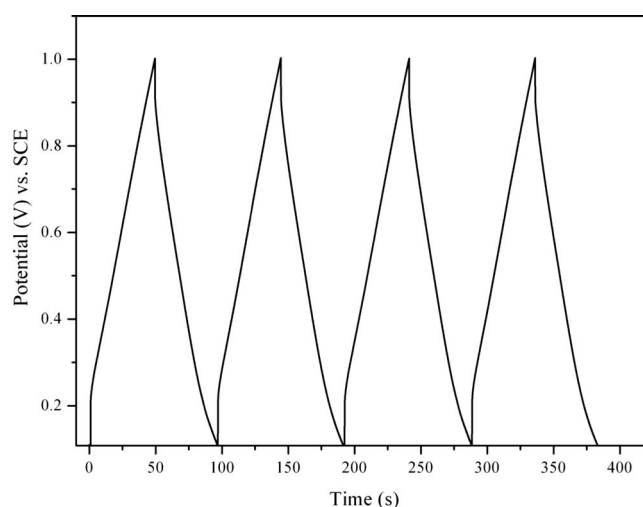
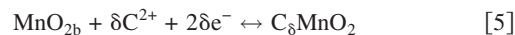


**Figure 3.** Charge-discharge curves of MnO<sub>2</sub> electrode in 0.1 mol L<sup>-1</sup> Mg(NO<sub>3</sub>)<sub>2</sub> at a current density of 4 A g<sup>-1</sup>.

The pseudo-capacitance of MnO<sub>2</sub> electrode in mild electrolytes containing alkaline-earth cations should be ascribed to the rapidly reversible insertion-extraction reaction



where C is Mg<sup>2+</sup>, Ca<sup>2+</sup>, or Ba<sup>2+</sup>.<sup>21,22</sup>

It is known that the bigger the cation size, the more difficult it is to squeeze and diffuse in the MnO<sub>2</sub> matrix. From a vacancy point of view, a higher storage capacity could be obtained as the guest cation with a smaller size. Thus, the highest specific capacitance of MnO<sub>2</sub> electrode in 0.1 M Mg(NO<sub>3</sub>)<sub>2</sub> within the potential range from 0.10 to 1.00 V vs SCE should ascribe to the smallest bare ions size of Mg<sup>2+</sup>, as shown in Table I.

Typical charge-discharge curves of MnO<sub>2</sub> electrode in 0.1 M Mg(NO<sub>3</sub>)<sub>2</sub> electrolyte at a current density of 4 A g<sup>-1</sup> are shown in Fig. 3. Although a sharp iR drop was found due to the poor conductivity of MnO<sub>2</sub> as well as the high current density, there is a linear variation of potential during charging and discharging processes, which is another criterion for capacitance behavior of a material in addition to exhibiting rectangular voltammograms. The rectangular-like CV curves and the linear variation of potential on times during charging and discharging processes from Fig. 2 and 3 indicate the ideal capacitive behavior of MnO<sub>2</sub> in aqueous electrolytes containing alkaline-earth cations.

The electrodes were subjected to extended charge-discharge cycling at a current density of 1 A g<sup>-1</sup> in the electrolytes containing alkaline-earth cations, and the result is shown in Fig. 4. No decrease in SC was found after 200 cycles, which shows that MnO<sub>2</sub> possesses a good cycling property in the aqueous electrolyte containing bivalent cations (Mg<sup>2+</sup>, Ca<sup>2+</sup>, or Ba<sup>2+</sup>). Moreover, for all electrolytes, the coulombic efficiency was nearly 100% during charge-discharge cycling tests, which indicates the high reversibility of MnO<sub>2</sub> toward cation intercalation in the potential range from 0.10 to 1.00 V vs SCE. The ideal capacitive behavior, higher specific capacitance, and good coulombic efficiency and rate ability of manganese dioxides in aqueous electrolytes containing bivalent cations (Mg<sup>2+</sup>, Ca<sup>2+</sup>, or Ba<sup>2+</sup>) indicate that these alkaline-earth cations might be good alternatives for the state-of-the-art univalent alkaline cations, which are widely used for MnO<sub>2</sub> supercapacitor applications.

The electrochemical impedance spectra were measured on the electrodes in 0.1 M Mg(NO<sub>3</sub>)<sub>2</sub>, Ca(NO<sub>3</sub>)<sub>2</sub>, and Ba(NO<sub>3</sub>)<sub>2</sub> electrolytes at 0.4 V vs SCE. Figure 5 shows the Nyquist plots of the experimental impedance data. All the measured impedance spectra are similar in shape with a semicircle in the higher-frequency region and a spark in the lower-frequency region. The measured

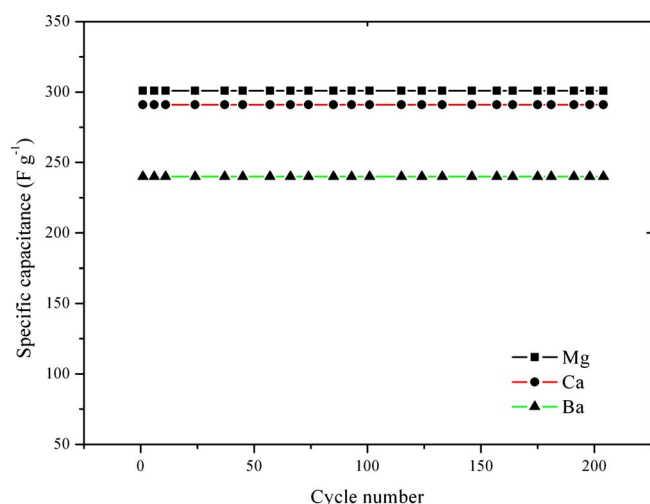


**Figure 4.** (Color online) Cycle lives of MnO<sub>2</sub> electrodes in all the electrolytes.

impedance data were analyzed on the basis of the equivalent circuit, which is shown in Fig. 5.<sup>26</sup> The model circuit consists of four elements: the internal resistance ( $R_s$ ), the constant phase element ( $Q$ ) used in place of double-layer capacitance ( $C_{dl}$ ), the charge-transfer resistance ( $R_{ct}$ ), and the Warburg impedance ( $Z_w$ ). The internal resistance ( $R_s$ ) includes the bulk electrolyte solution resistance, the intrinsic resistance of active material, and the electron-transfer resistance at the current collector/electrode boundary. The constant phase element ( $Q$ ) is used in place of double-layer capacitance ( $C_{dl}$ ) at the electrode–electrolyte boundary because the non-ideal nature of capacitance arises due to the inhomogeneous nature of the electrode. The charge-transfer resistance ( $R_{ct}$ ) represents the kinetic resistance to charge transfer at the electrode–electrolyte boundary or intrinsic charge-transfer resistance of the solution and porous electrode. The Warburg impedance ( $Z_w$ ) associates with the finite-length diffusion of cation in the solid particle.

The fitting results as well as the diffusion coefficient of alkaline-earth cations in the as-prepared MnO<sub>2</sub> particles are listed in Table II. The value of  $R_{ct}$  for 0.1 M Mg(NO<sub>3</sub>)<sub>2</sub>, Ca(NO<sub>3</sub>)<sub>2</sub>, and Ba(NO<sub>3</sub>)<sub>2</sub> electrolytes are 13.36, 9.10, and 11.48, respectively. It can be seen from Tables I and II that  $R_{ct}$  values decrease with the decrease in

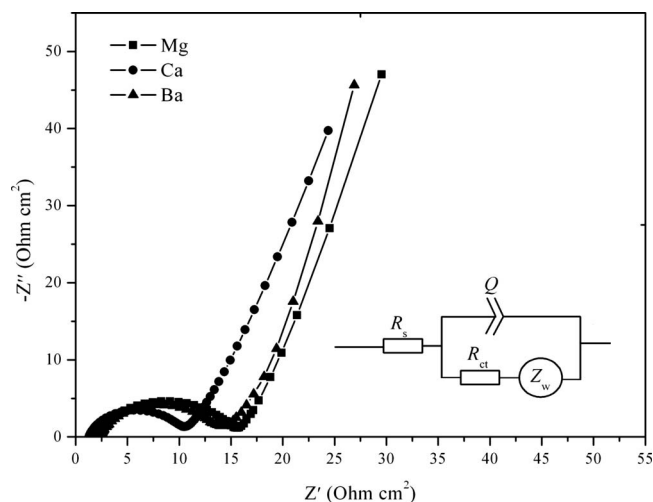


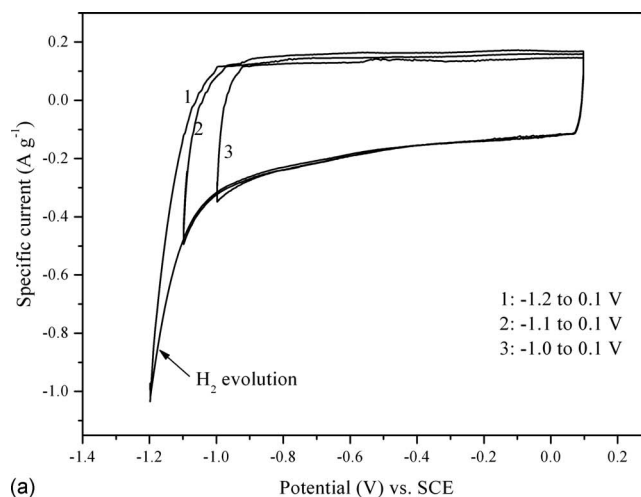
**Figure 5.** Nyquist plots of MnO<sub>2</sub> electrode in 0.1 mol L<sup>-1</sup> Mg(NO<sub>3</sub>)<sub>2</sub>, Ca(NO<sub>3</sub>)<sub>2</sub>, and Ba(NO<sub>3</sub>)<sub>2</sub> electrolytes. Insert shows the equivalent circuit.

**Table II.** The calculated values of,  $C_{dl}$ ,  $R_{ct}$ , and diffusion coefficient of MnO<sub>2</sub> electrodes in the aqueous electrolytes containing the listed cations.

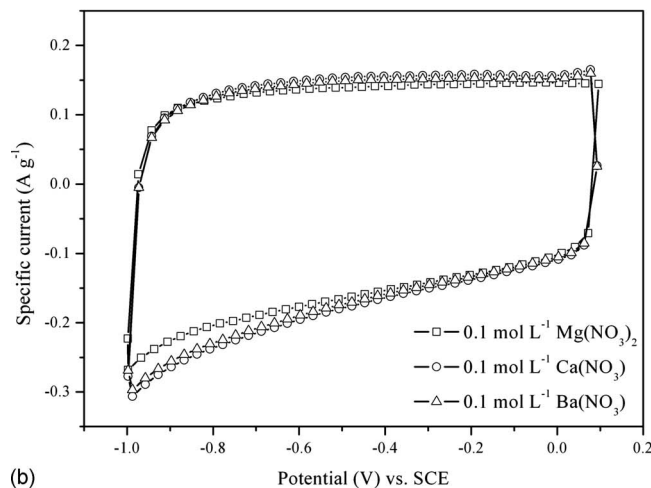
Cation species	$R_s$ ( $\Omega$ )	$C_{dl}$ (mF)	$R_{ct}$ ( $\Omega$ )	Diffusion coefficient ( $\times 10^{-14}$ cm <sup>2</sup> s <sup>-1</sup> )
Mg	2.10	0.14	13.36	10.81
Ca	1.50	0.30	9.10	8.70
Ba	2.26	0.16	11.48	7.41

size of hydrated cations. The diffusion coefficient of Mg<sup>2+</sup>, Ca<sup>2+</sup>, and Ba<sup>2+</sup> are 10.81, 8.70, and 7.41  $\times 10^{-14}$  cm<sup>2</sup> s<sup>-1</sup>, respectively. These values are compared to  $1.00 \times 10^{-13}$  cm<sup>2</sup> s<sup>-1</sup> of the univalent lithium ions and  $3.05 \times 10^{-15}$  cm<sup>2</sup> s<sup>-1</sup> of the trivalent yttrium ions in nanocrystalline transition-metal oxide (V<sub>2</sub>O<sub>5</sub>).<sup>27</sup>

**Electrochemical properties of AC.**— A commercial AC (Kuraray Company, Japan) was used in this work. The  $S_{BET}$  value is 1620 m<sup>2</sup> g<sup>-1</sup> and the total pore volume is 0.8 cm<sup>3</sup> g<sup>-1</sup>. In order to obtain a high cell operating potential, the potential range of AC has to be controlled elaborately. Because the minimum cutoff of MnO<sub>2</sub> electrodes is 0.10 V vs SCE for all electrolytes, the positive polarization cutoff of AC electrodes is set to be 0.10 V vs SCE. Figure 6a shows the CV of AC in 0.1 M Ca(NO<sub>3</sub>)<sub>2</sub> (pH 6.0) at different nega-



(a)



(b)

**Figure 6.** CVs of AC electrodes: (a) in 0.1 mol L<sup>-1</sup> Ca(NO<sub>3</sub>)<sub>2</sub> at different minimal cutoffs and (b) in all the electrolytes within the potential range from -1.0 to 0.1 V vs SCE.

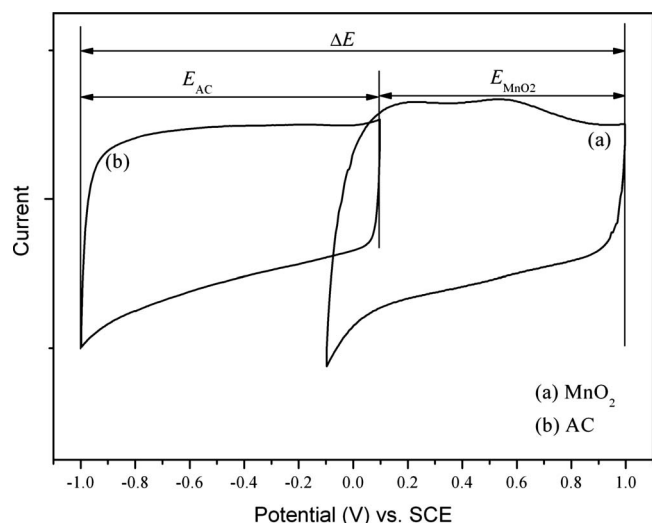


**Figure 7.** Schematic graph of the cell operating potential range using 0.1 mol L<sup>-1</sup> Ca(NO<sub>3</sub>)<sub>2</sub> electrolytes.

tive polarization cutoffs. The rectangular shape of the CV down to a potential cutoff of  $-1.00$  V with similar positive and negative current proves a pure reversible capacitive behavior in this potential range. As the potential became more negative ca.  $-1.20$  V, the evolution of water was also clearly observed. Figure 6b exhibits the CVs of AC electrodes in all electrolytes at a scan rate of  $2 \text{ mV s}^{-1}$ . The mirrorlike CV indicates the double-layer capacitive behavior of the AC electrodes in all electrolytes. The SC values of AC in 0.1 M Mg(NO<sub>3</sub>)<sub>2</sub>, Ca(NO<sub>3</sub>)<sub>2</sub>, and Ba(NO<sub>3</sub>)<sub>2</sub> electrolytes calculated from Eq. 2 are 72, 80, and 76 F g<sup>-1</sup>, respectively. The lowest SC of AC in 0.1 M Mg(NO<sub>3</sub>)<sub>2</sub> electrolyte could be attributed to the largest hydrated ion size of Mg<sup>2+</sup> because the AC utilizes the electrochemical double-layer mechanism, in which the anions and cations were absorbed-desorbed on the surface of the inner pores.

The above results provide a firm basis to build up the asymmetric capacitors by the combination of MnO<sub>2</sub> and AC in the aqueous electrolytes containing alkaline-earth cations. The schematic graph of the cell operating potential range using 0.1 M Ca(NO<sub>3</sub>)<sub>2</sub> electrolytes is shown in Fig. 7. The potential range of positive MnO<sub>2</sub> electrode has to be controlled at 0.10 to 1.00 V vs SCE, in which the reversible reaction occurs. The AC electrode shows a unique behavior under negative polarization with a high hydrogen overpotential, and the potential range of AC could be set to  $-1.00$  to 0.10 V vs SCE.

In order to obtain the maximal cell operating voltage, the loading mass of positive and negative electrodes has to be balanced. For this purpose, it must be considered that the charges at positive ( $q_+$ ) and negative ( $q_-$ ) electrodes should be balanced to be equal. The charge stored by each electrode depends on the specific capacitance ( $C$ ), the potential range for the charge/discharge process ( $\Delta E$ ), and the mass of the electrode ( $m$ ) as in the following equation<sup>13</sup>

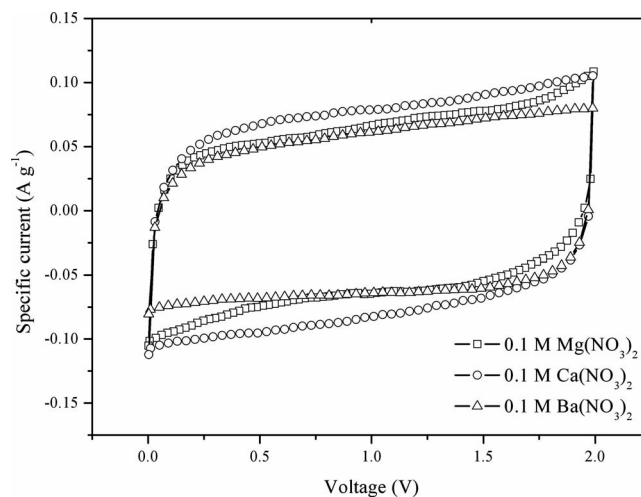


**Figure 8.** CVs of the asymmetric capacitors using different electrolytes at  $2 \text{ mV s}^{-1}$ .

$$q = C \times \Delta E \times m \quad [6]$$

and in order to get  $q_+ = q_-$ , the mass balancing is

$$m_+/m_- = C_- \times \Delta E_- / C_+ \times \Delta E_+ \quad [7]$$

On the basis of the specific capacitance values and potential ranges found at pH 6.0 for the manganese oxide composite and AC, the optimal mass ratios in all electrolytes between the electrodes is listed in Table III.

*Electrochemical performance of AC/MnO<sub>2</sub> asymmetric capacitors.*— The asymmetric cells were built up according to the mass ratio listed in Table III. The CVs of the asymmetric cells using 0.1 M Mg(NO<sub>3</sub>)<sub>2</sub>, Ca(NO<sub>3</sub>)<sub>2</sub>, and Ba(NO<sub>3</sub>)<sub>2</sub> electrolytes are shown in Fig. 8 at  $2 \text{ mV s}^{-1}$  in the potential range from 0 to 2 V. These CVs are generally rectangular, which indicates that no other irreversible reactions occur in this voltage range, and a high voltage of AC/MnO<sub>2</sub> supercapacitors using the aqueous electrolytes containing the alkaline-earth cations (Mg<sup>2+</sup>, Ca<sup>2+</sup>, or Ba<sup>2+</sup>) could be obtained.

The capacitance (SC) of the asymmetric supercapacitors can be estimated using half the integrated area of the CV curve to obtain the charge ( $Q$ ) and subsequently dividing the charge by the total mass of the positive and negative active materials ( $M$ ) and the width of the potential window ( $\Delta V$ )

$$SC = Q/\Delta VM \quad [8]$$

At a low scan rate of  $2 \text{ mV s}^{-1}$ , the SC values of the asymmetric cells with aqueous electrolytes containing Mg<sup>2+</sup>, Ca<sup>2+</sup>, or Ba<sup>2+</sup> cations are 37, 32, and 29 F g<sup>-1</sup>, respectively. It is known that the electrochemical performance of an asymmetric supercapacitor depends on both negative and positive electrodes. The above single electrode characterizations indicated that due to the largest bare ion size of Ba<sup>2+</sup> cation, the SC value, 281 F g<sup>-1</sup> of the positive MnO<sub>2</sub> in 0.1 M Ba(NO<sub>3</sub>)<sub>2</sub> electrolytes is 15 or 12% less than 325 F g<sup>-1</sup> in

**Table III.** Summaries of the properties of positive and negative electrodes in three electrolytes containing different cations.

Cation species	Positive MnO <sub>2</sub> electrode		Negative AC electrode		Mass ratio
	SC (F g <sup>-1</sup> )	Potential window (V)	SC (F g <sup>-1</sup> )	Potential window (V)	
Mg	325	0.9	72	1.1	3.69
Ca	314	0.9	80	1.1	3.17
Ba	281	0.9	76	1.1	3.03

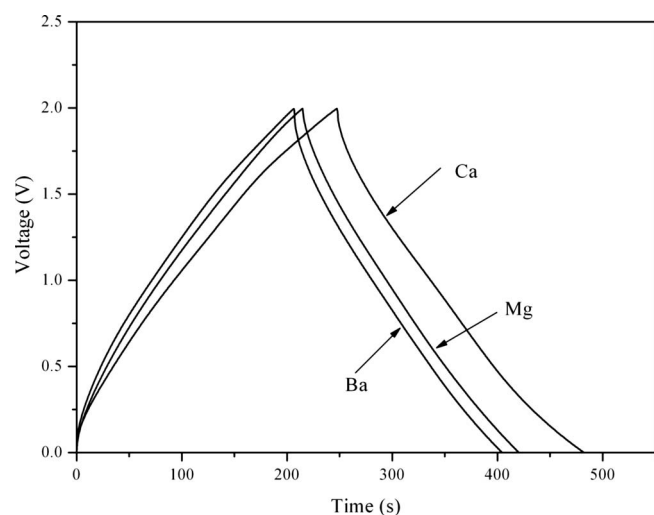


**Figure 9.** Charge–discharge curves of the asymmetric capacitors using different electrolytes at  $0.3 \text{ A g}^{-1}$ .

$0.1 \text{ M Mg(NO}_3)_2$  electrolyte or  $314 \text{ F g}^{-1}$  in  $0.1 \text{ M Ca(NO}_3)_2$  electrolyte. Although the SC value ( $76 \text{ F g}^{-1}$ ) of negative AC electrode in  $0.1 \text{ M Ba(NO}_3)_2$  is higher than  $72 \text{ F g}^{-1}$  in  $0.1 \text{ M Mg(NO}_3)_2$  electrolyte, this slight enhancement on the negative electrodes could not average the large gap between the SC values of the positive  $\text{MnO}_2$  electrodes. Therefore, the cell with  $0.1 \text{ M Ba(NO}_3)_2$  electrolyte exhibited the lowest capacitance. Comparing the  $\text{Mg}^{2+}$  cation with  $\text{Ca}^{2+}$  cation, despite that the positive SC value in  $0.1 \text{ M Mg(NO}_3)_2$  electrolyte is slightly higher than in  $0.1 \text{ M Ca(NO}_3)_2$  electrolyte, there is the largest difference between positive and negative SC values when  $0.1 \text{ M Mg(NO}_3)_2$  electrolyte is used, which means the largest total mass of both positive and negative active materials, as shown in Table III. In addition, the smallest SC value of negative electrode also prevented the AC/ $\text{MnO}_2$  cell with  $\text{Mg}^{2+}$  cation from reaching the highest capacitance. It seems that due to the appropriate bare ion size and the smallest hydrated ion size among three alkaline-earth cations ( $\text{Mg}^{2+}$ ,  $\text{Ca}^{2+}$ , and  $\text{Ba}^{2+}$ ),  $\text{Ca}^{2+}$  ion is suitable for the asymmetric AC/ $\text{MnO}_2$  supercapacitor.

Figure 9 shows the charge–discharge curves of the asymmetric cells using  $0.1 \text{ M Mg(NO}_3)_2$ ,  $\text{Ca(NO}_3)_2$ , and  $\text{Ba(NO}_3)_2$  electrolytes at  $0.3 \text{ A g}^{-1}$  (taking into account only the total weight of positive and negative active materials). The potentials are nearly proportional to the charge or discharge time for all the electrolytes containing  $\text{Mg}^{2+}$ ,  $\text{Ca}^{2+}$ , or  $\text{Ba}^{2+}$  cations. It is seen from Fig. 8a and 9a that during charging between 0 and 2 V, for all asymmetric cells using aqueous electrolytes containing  $\text{Mg}^{2+}$ ,  $\text{Ca}^{2+}$ , or  $\text{Ba}^{2+}$  cations, irreversible faradaic processes such as dissolution of  $\text{Mn}^{2+}$  and oxygen or hydrogen evolution reaction seem to be avoided.

Figure 10 exhibits the Ragone plots of the three asymmetric cells with the aqueous electrolytes containing  $\text{Mg}^{2+}$ ,  $\text{Ca}^{2+}$ , or  $\text{Ba}^{2+}$  cations. Because the packaging is not taken into account and all the cell components are not yet optimized, these data only provide an estimation of the performance of the capacitors. The Ragone plot data clearly demonstrates that AC/ $\text{MnO}_2$  asymmetric systems in mild aqueous electrolytes containing alkaline-earth cations can compete with the organic electrolyte-based carbon capacitors,<sup>2,3</sup>  $\text{RuO}_2$  capacitors,<sup>1,28</sup> or AC/ $\text{MnO}_2$  with aqueous electrolytes containing alkaline cations,<sup>12–15</sup> although the SC value of the negative AC electrode is much smaller than those in Ref. 12–15. For example, the real energy density of AC/ $\text{MnO}_2$  using  $0.1 \text{ M Ca(NO}_3)_2$  electrolyte was  $21 \text{ Wh Kg}^{-1}$  at a power density of  $300 \text{ W Kg}^{-1}$  for a cutoff voltage of 0–2 V.

The cycling stability of all the asymmetric cells was tested over 5000 cycles. The cutoff voltage of all the asymmetric cells is con-

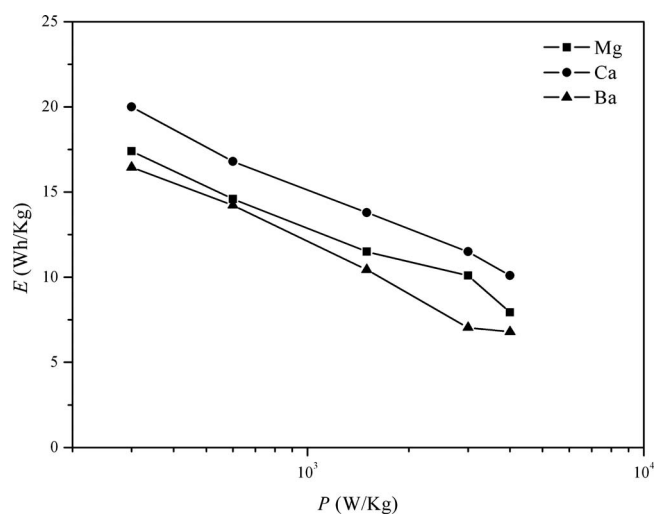


**Figure 10.** Ragone plots of the asymmetric capacitors using different cations.

trolled from 0 to 2 V at a current density of  $0.3 \text{ A g}^{-1}$ . The variations of specific capacitances of all the cells and the coulombic efficiency of the AC/ $\text{Mg(NO}_3)_2$ / $\text{MnO}_2$  cell during cycling are illustrated in Fig. 11. All the asymmetric cells exhibited good cycle ability in terms of capacitance retention and the coulombic efficiency.

### Conclusion

Manganese dioxide was assessed to exhibit the ideal capacitive behavior in aqueous electrolytes containing alkaline-earth cations ( $\text{Mg}^{2+}$ ,  $\text{Ca}^{2+}$ , or  $\text{Ba}^{2+}$ ). The ideal capacitive behavior, higher specific capacitance, and good coulombic efficiency and rate ability of manganese dioxides in aqueous electrolytes containing bivalent cations ( $\text{Mg}^{2+}$ ,  $\text{Ca}^{2+}$ , or  $\text{Ba}^{2+}$ ) indicated that these alkaline-earth cations might be good alternatives for the state-of-the-art univalent alkaline cations, which are widely used for  $\text{MnO}_2$  supercapacitor applications. The AC/ $\text{MnO}_2$  asymmetric capacitors with 2 V operating voltage were built up based on the aqueous electrolytes containing these alkaline-earth cations. The energy density of the AC/ $\text{MnO}_2$  asymmetric capacitor with  $\text{Ca}^{2+}$  cation at a current density of  $0.3 \text{ A g}^{-1}$  was found to be  $21 \text{ Wh Kg}^{-1}$ , which is comparable to that of the  $\text{RuO}_2$  capacitor or organic-based carbon symmetric capacitor. It was also found that due to the appropriate bare ion size and the

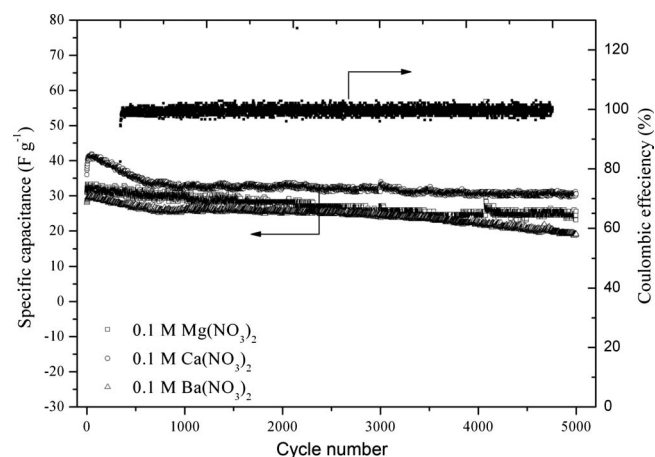


**Figure 11.** Cycle lives of all the asymmetric capacitors using different cations.

smallest hydrated ion size among three alkaline-earth cations ( $\text{Mg}^{2+}$ ,  $\text{Ca}^{2+}$ , and  $\text{Ba}^{2+}$ ),  $\text{Ca}^{2+}$  cation is suitable for the asymmetric AC/ $\text{MnO}_2$  supercapacitor.

#### Acknowledgment

This work was supported by the Natural Science Foundation of China under grant no. 50632040 and no. 50802049.

Tsinghua University assisted in meeting the publication cost of this article.

#### References

1. B. E. Conway, *Electrochemical Supercapacitors, Scientific Fundamentals and Technological Applications*, Kluwer Academic/Plenum Press, New York (1999).
2. J. P. Zheng and T. R. Jow, *J. Electrochem. Soc.*, **144**, 2417 (1997).
3. M. Mastragostino, C. Arbizzani, R. Paraventi, and A. Zanelli, *J. Electrochem. Soc.*, **147**, 407 (2000).
4. R. Kotz and M. Carlen, *Electrochim. Acta*, **45**, 2483 (2000).
5. P. L. Taberna, P. Simon, and J. F. Fauvarque, *J. Electrochem. Soc.*, **150**, A292 (2003).
6. J. P. Zheng and T. R. Jow, *J. Electrochem. Soc.*, **142**, L6 (1995).
7. J. P. Zheng and T. R. Jow, *J. Power Sources*, **62**, 155 (1996).
8. J. H. Park, O. O. Park, K. H. Shin, C. S. Jin, and J. H. Kim, *Electrochem. Solid-State Lett.*, **5**, H7 (2002).
9. A. I. Beliakov and A. M. Brintsev, in *Proceedings of the 7th International Seminar on Double Layer Capacitors and Similar Energy Storage Devices*, Florida Educational Seminars (1997).
10. Y. Wang and Y. Xia, *J. Electrochem. Soc.*, **153**, A450 (2006).
11. Y. Wang and Y. Xia, *J. Electrochem. Soc.*, **153**, A1425 (2006).
12. M. S. Hong, S. H. Lee, and S. W. Kim, *Electrochem. Solid-State Lett.*, **5**, A227 (2002).
13. V. Khomenko, E. Raymundo-Piñero, and F. Bèguin, *J. Power Sources*, **153**, 183 (2006).
14. T. Brousse, M. Toupin, and D. Bélanger, *J. Electrochem. Soc.*, **151**, A614 (2004).
15. T. Brousse, P. L. Taberna, O. Crosnier, R. Dugas, P. Guillemet, Y. Scudeller, Y. Zhou, F. Favier, D. Bélanger, and P. Simon, *J. Power Sources*, **173**, 633 (2007).
16. S.-C. Pang, M. A. Anderson, and T. W. Chapman, *J. Electrochem. Soc.*, **147**, 444 (2000).
17. M. Toupin, T. Brousse, and D. Belanger, *Chem. Mater.*, **16**, 3186 (2004).
18. C.-C. Hu and T.-W. Tsou, *Electrochem. Commun.*, **4**, 105 (2002).
19. M. Toupin, T. Brousse, and D. Bélange, *Chem. Mater.*, **14**, 946 (2002).
20. J. Rishpon and S. Gottesfield, *J. Electrochem. Soc.*, **131**, 1960 (1984).
21. C.-C. Hu, T.-T. Wu, and K.-H. Chang, *Chem. Mater.*, **20**, 2893 (2008).
22. C. Xu, H. Du, B. Li, F. Kang, and Y. Zeng, *J. Electrochem. Soc.*, **156**, A73 (2009).
23. J. A. Dean, *Lange's Handbook of Chemistry*, McGraw-Hill, New York (1992).
24. C. Xu, B. Li, H. Du, F. Kang, and Y. Zeng, *J. Power Sources*, **180**, 664 (2008).
25. C. Xu, B. Li, H. Du, F. Kang, and Y. Zeng, *J. Power Sources*, **184**, 691 (2008).
26. C. Ho, I. D. Raistrick, and R. A. Huggins, *J. Electrochem. Soc.*, **127**, 343 (1980).
27. G. G. Amatucci, F. Badway, A. Singhal, B. Beaudoin, G. Skandan, T. Bowmer, I. Plitz, N. Pereira, T. Chapman, and R. Jaworski, *J. Electrochem. Soc.*, **148**, A940 (2001).
28. A. Burke, *J. Power Sources*, **91**, 37 (2000).